Süleyman Demirel Üniversitesi
Fen Bilimleri Enstitüsü Dergisi
Cilt 30, Sayı 2, 262-279, 2026

Süleyman Demirel University
Journal of Natural and Applied Sciences
Volume 30, Issue 2, 262-279, 2026

DOI: 10.19113/sdufenbed.1719916

Theoretical Investigation of the *N*-(4-(4-chlorophenyl)oxazol-2-yl)-4-phenyl-1*H*-pyrazole-3-carboxamide Molecule by DFT Method and Molecular Docking Evaluation Against SARS-CoV-2 Main Proteases

Barış KARTAL[1], Kenan GÖREN[2*], Mehmet BAĞLAN[3], Ümit YIDIKO[4]

[1]Adıyaman Üniversitesi, Gölbaşı Meslek Yüksekokulu, Mülkiyet Koruma ve Güvenlik Dairesi Başkanlığı, Adıyaman, Türkiye
[2]Şırnak Üniversitesi, Mühendislik Fakültesi, Petrol ve Doğalgaz Mühendisliği Bölümü, 73000, Şırnak, Türkiye
[3]Kafkas Üniversitesi, Fen ve Edebiyat Fakültesi, Kimya Bölümü, 36000, Kars, Türkiye
[4]Kafkas Üniversitesi, Mühendislik Fakültesi, Biyomühendislik Bölümü, 36000, Kars, Türkiye

(Alınış / Received: 14.06.2025, Kabul / Accepted: 02.06.2026, Online Yayınlanma / Published Online: 25.08.2026)

Keywords
DFT
Molecular Docking
ADME
MEP
NBO
Benzoxazole

Abstract: In this study, *N*-(4-(4-chlorophenyl)oxazol-2-yl)-4-phenyl-1*H*-pyrazole-3-carboxamide (NOPC), a benzoxazole derivative with potential biological activity, was investigated in detail by theoretical and computational methods. The structural and electronic properties of the molecule were analyzed usinsg the 6-31G(d,p) basis set with B3LYP and PBEPBE methods within the scope of Density Functional Theory (DFT). In this context, optimized geometry, HOMO-LUMO energy levels, NBO analysis, Mulliken charge distribution, NLO properties and MEPS surface were evaluated. In addition, the interaction of the NOPC molecule with 6W75 and 7BV2, the main proteases of the SARS-CoV-2 virus, was investigated by molecular docking method, and binding energies of -7.70 and -8.40 kcal/mol were obtained, respectively. These findings indicate that the molecule exhibits strong binding affinity and may be a potential inhibitor against COVID-19. Finally, ADME analyses performed with ADMETlab 2.0 revealed that NOPC complies with Lipinski rules and has high oral bioavailability potential. The obtained data indicate that NOPC molecule is a promising candidate for drug design.

N-(4-(4-Klorofenil)oksazol-2-il)-4-fenil-1*H*-pirazol-3-karboksamid Molekülünün DFT Yöntemiyle Teorik İncelenmesi ve SARS-CoV-2 Ana Proteazlarına Karşı Moleküler Doking Değerlendirilmesi

Anahtar Kelimeler
DFT
Moleküler Doking
ADME
MEP
NBO
Benzoksazol

Öz: Bu çalışmada, potansiyel biyolojik aktiviteye sahip bir benzoksazol türevi olan *N*-(4-(4-klorofenil)oksazol-2-il)-4-fenil-1*H*-pirazol-3-karboksamid (NOPC) molekülü teorik ve hesaplamalı yöntemlerle detaylı olarak incelenmiştir. Molekülün yapısal ve elektronik özellikleri, Yoğunluk Fonksiyonel Teorisi (DFT) kapsamında B3LYP ve PBEPBE metotları ile 6-31G(d,p) temel seti kullanılarak analiz edilmiştir. Bu kapsamda optimize geometri, HOMO-LUMO enerji seviyeleri, NBO analizi, Mulliken yük dağılımı, NLO özellikleri ve MEPS yüzeyi değerlendirilmiştir. Ayrıca, NOPC molekülünün SARS-CoV-2 virüsünün ana proteazları olan 6W75 ve 7BV2 ile etkileşimi moleküler doking yöntemiyle araştırılmış, sırasıyla -7,70 ve -8,40 kcal/mol bağlanma enerjileri elde edilmiştir. Bu bulgular, molekülün güçlü bağlanma afinitesi gösterdiğini ve COVID-19'a karşı potansiyel bir inhibitör olabileceğini göstermektedir. Son olarak, ADMETlab 2.0 ile yapılan ADME analizleri, NOPC'nin Lipinski kurallarına uygun olduğunu ve yüksek oral biyoyararlanım potansiyeline sahip olduğunu ortaya koymuştur. Elde edilen veriler, NOPC molekülünün ilaç tasarımı açısından umut vadeden bir aday olduğunu göstermektedir.

1. Introduction

Heterocyclic compounds, which are cyclic organic structures containing at least one heteroatom such as nitrogen, oxygen, or sulfur, are of great importance in

*Corresponding author: kenangoren49@gmail.com

contemporary drug design and development. This class of compounds has a high importance in pharmaceutical chemistry due to its chemical diversity and potential to interact with biological targets [1, 2]. In particular, natural and synthetic derivatives exhibit activity in a very wide pharmacological spectrum such as antimicrobial, anticancer, antiviral, antifungal, anti-inflammatory and central nervous system agents [3, 4]. The broad spectrum of biological activities exhibited by heterocyclic systems arises from their capacity to interact with specific binding regions of molecular targets and to efficiently facilitate molecular recognition. In this context, the benzoxazole nucleus, which is formed by the fusion of the benzene ring and the oxazole ring, is a structure that draws attention with both its aromatic character and polypharmacological potential. Benzoxazole derivatives have been extensively demonstrated in the literature to have numerous biological activities, including antibacterial, antifungal, antitumor, antituberculosis and antiviral effects [5]. The pharmacological effects of such structures can generally be modulated by various functional groups attached to the core structure. This makes the benzoxazole skeleton an attractive structural platform for the design of new therapeutic agents [6].

In recent years, the global outbreak of Coronavirus disease 2019 (COVID-19) has represented a significant public health challenge, prompting intensified research efforts toward the discovery and development of novel antiviral agents. The disease is caused by SARS-CoV-2, an enveloped, positive-sense single-stranded RNA virus that was first detected in Wuhan, China, in December 2019 and rapidly evolved into a worldwide crisis [7]. The World Health Organization (WHO) declared COVID-19 a public health emergency of international concern on January 30, 2020, and a global pandemic on March 11, 2020. The rapid spread and impact of the outbreak have been influenced by some critical epidemiological factors, such as the ability of infected individuals to transmit the virus before showing symptoms. A better understanding of SARS-CoV-2 at the molecular level is vital for the development of Effective medical care strategies and antiviral compounds [8].

At this stage, computational chemistry approachesparticularly DFT have emerged as powerful tools for investigating the structural and electronic characteristics of biologically active molecules [9]. DFT is widely preferred in theoretical chemistry due to its ability to predict the ground state energies, molecular orbitals, charge distributions, and reactivity indices of molecules with high accuracy and in a cost-effective manner. This method is used in molecular modeling studies, especially to predict the potential biological activities of new compounds and to evaluate molecule-target interactions [9].

Recent research has emphasized the promise of heterocyclic frameworks, particularly oxazole and pyrazole derivatives, as potential antiviral agents targeting coronaviruses. Notably, several macrocyclic compounds containing oxazole units have demonstrated inhibitory activity against the SARS-CoV-2 main protease (Mpro) in both in vitro and cellular assays, supported by molecular docking studies that reveal favorable interactions within the enzyme's active site [10]. Additionally, pyrazole derivatives bearing hydroxyquinoline scaffolds have demonstrated significant antiviral activity against SARS-CoV-2 and other coronaviruses (MERS-CoV, HCoV-229E), with molecular docking studies supporting their interaction with key viral proteins, as well as pharmacokinetic profiles compatible with drug-like properties [11]. A broader review of heterocyclic compounds further indicates that both oxazole and pyrazole motifs are recurrently identified among diverse small molecules investigated for anti-SARS-CoV-2 activity *in vitro* and *in silico* [12]. However, most of these reports focus on either individual heterocyclic units or simpler analogs, and relatively few studies have integrated comprehensive electronic structure analysis, pharmacokinetic evaluation, and molecular docking for structurally hybrid systems. In this context, the NOPC molecule, which incorporates both oxazole and pyrazole rings connected via a carboxamide linker, represents a unique hybrid scaffold whose detailed theoretical evaluation against SARS-CoV-2 targets has not been previously reported.

In this study, the compound *N*-(4-(4-chlorophenyl)oxazol-2-yl)-4-phenyl-1*H*-pyrazole-3-carboxamide (NOPC) [5], which carries a benzoxazole ring in its structure and is evaluated as a potential antiviral agent candidate, was comprehensively investigated by theoretical calculations and molecular modeling approaches. The structural optimization of the compound was performed by DFT using B3LYP and PBEPBE methods, the pharmacokinetic profile was evaluated by ADME analyses, and the possible inhibitory effect against the SARS-CoV-2 virus was investigated through molecular docking simulations. Such theoretical studies provide scientific contributions to the development of rapid and effective treatment strategies against global health threats such as COVID-19.

2. Materials and Methods

Quantum chemical calculations of NOPC molecule were performed within the scope of density functional theory (DFT) using Gaussian 09 software package [13]. All calculations were carried out using the B3LYP

and PBEPBE density functional methods in conjunction with the 6-31G(d,p) basis set. These methods are widely used and have been demonstrated to provide reliable results for molecular geometries and electronic properties. The 6-31G(d,p) basis set was chosen as it offers a good balance between computational cost and accuracy, while the inclusion of polarization functions allows for an improved description of electron distribution and bonding characteristics. Three-dimensional crystal structures of target proteins were obtained from Protein Data Bank (PDB) [14]. Molecular docking studies were performed using the Glide module implemented in Schrödinger Maestro software (version 11.8) [15]; to investigate the binding affinity and interaction modes of the NOPC molecule with the active sites of the target proteins. The receptor grid was generated by centering on the co-crystallized ligand present in the active site of each protein. The grid box dimensions were set to [20×20×20 Å] to adequately encompass the binding pocket and allow sufficient ligand flexibility. Docking calculations were carried out using the Glide Standard Precision (SP) scoring function, and the most favorable binding poses were selected based on Glide docking scores and interaction profiles. To validate the docking protocol, the co-crystallized ligand was re-docked into the active site of the corresponding protein, and the root-mean-square deviation (RMSD) between the experimental and re-docked ligand conformations was calculated using the MOE (Molecular Operating Environment) program **[16]**. An RMSD value of less than 2.0 Å was obtained, indicating good agreement with the crystallographic binding mode and confirming the reliability of the docking procedure. The resulting ligand–protein complexes were thoroughly examined using Discovery Studio Visualizer (version 2016) [17] to identify key interactions such as hydrogen bonding, hydrophobic contacts, and π–π interactions, and to elucidate the structural features of the binding modes. Interaction types (hydrogen bonds, hydrophobic interactions, etc.) were visualized and the binding mode of the molecule was structurally interpreted. The pharmacokinetic properties and drug candidacy potential of NOPC molecule were evaluated using the ADMETlab 2.0 online platform (https://admetmesh.scbdd.com/). Absorption, distribution, metabolism, and excretion (ADME) parameters were analyzed. In this context, important parameters such as Lipinski rules, gastrointestinal absorption, blood-brain barrier permeability, and interaction potential with CYP3A4 enzymes were taken into consideration.

3. Results and Discussion

3.1. Structure details and analysis

Geometry optimization aims to find the lowest energy configuration of a molecule or material. This type of optimization allows the system to become more stable and more accurate results to be obtained [18, 19]. Software such as Gaussian-09 [13], together with such optimization processes, is effective in calculating molecular orbitals, bond energies, charge distributions and many other important physicochemical properties [20]. Correct modeling of structural and electronic properties of pharmaceutical compounds is critical for drug design and understanding of their mechanisms of action [21]. In this study, molecular geometry optimization of a pharmaceutically important compound was performed using B3LYP and PBEPBE methods and calculations were carried out with 6-31G(d,p) basis set. The obtained data revealed that functional choices had significant effects on bond lengths, bond angles and planar angles. Particularly, structural differences around the active site indicate potential structural variations that may directly affect the interaction profile of the compound with target proteins and its biological activity. These results indicate that theoretical calculations can provide significant contributions in early-stage drug discovery processes, especially in the evaluation of molecular interactions and conformational conformations. Bond lengths, bond angles and planar bond angles in B3LYP and PBEPBE methods have been given in Table 1. Optimized geometric parameters show significant changes when both methods are used. First, C11-C12 bond length is 1.49135 Å with B3LYP functional, while it decreases to 1.43376 Å with PBEPBE functional. Similarly, C15-O16 bond length is found to be 1.41430 Å with B3LYP and 1.37112 Å with PBEPBE. Such changes are related to how the functionals used model the electron density differently. These bond length changes give crucial hints about the stability and reactivity of the molecule. Bond angles also reflect the differences between both methods. C17-C18-C20 bond angle is calculated as 130.74091° with B3LYP, while this angle decreases to 129.94430° with PBEPBE. Similarly, the C8-N9-N10 bond angle was found to be 113.28330° with B3LYP and 107.22671° with PBEPBE. The O13-C12-N14 bond angle was calculated as 119.41905° with B3LYP and 115.10687° with PBEPBE. The changes between these bond angles are a result of the fact that both functionals handle the electron density between the bonds differently. Planar bond angles are of critical importance, especially in understanding the in-plane structure of the molecule and the relationships between atoms. The C2-C3-C4-C7 planar bond angle was calculated as -177.58703° with B3LYP and 176.40643° with PBEPBE. Similarly, the O16-C17-C18-C20 planar bond angle was found to be 179.92739° with B3LYP and -179.56154° with PBEPBE. The large changes in these angles are due to the fact that the functionals used model the planar symmetry of the bond between the atoms differently.

Figure 1 shows the geometric representation of the NOPC compound optimized by the B3LYP method.

The calculated geometric parameters show that the structural properties of NOPC are generally consistent with the values reported in the literature for similar oxazole and pyrozole derivatives. The C–C bond lengths in the aromatic rings (C1–C2=1.395 Å, C4–C5=1.405 Å) were found to be in the range of 1.39–1.41 Å at both levels of calculation, which is consistent with typical C–C bond lengths in similar aromatic and heteroaromatic systems [22]. The calculated C11–N10 (1.338 Å) and C8–N9 (1.356 Å) bond lengths in the pyrosol core of NOPC also show good comparison with the 1.33–1.38 Å range reported in the literature for pyrosol and pyrazolo derivatives[23].

Table 1. The NOPC molecule's theoretically determined bond lengths (Å) and bond angles (°).

Bond Lengths	B3LYP	PBEPBE	Bond Lengths	B3LYP	PBEPBE
C1-C2	1.39581	1.40202	C12-O13	1.22478	1.24881
C4-C5	1.40489	1.41117	C15-O16	1.41430	1.37112
C4-C7	1.47818	1.47733	C12-N14	1.39027	1.45677
C7-C11	1.43561	1.44636	C11-N10	1.33825	1.40750
C11-C12	1.49135	1.43376	C8-N9	1.35640	1.38504
C17-C18	1.35160	1.36949	C23-CI26	1.75822	1.75537
Bond Angles	B3LYP	PBEPBE	Bond Angles	B3LYP	PBEPBE
C1–C2-C3	120.04235	120.02479	C8-N9-NI0	113.28330	107.22671
C5-C4-C7	122.53490	122.52055	O13-C12-N14	119.41905	115.10687
C7-C11-C12	128.94737	128.98903	O16-C15-N19	107.05023	114.01142
C17-C18-C20	130.74091	129.94430	C22-C23-CI26	119.48292	119.46420
Planar Bond Angles	B3LYP	PBEPBE	Planar Bond Angles	B3LYP	PBEPBE
C2-C3-C4-C7	-177.58703	176.40643	N14-C15-N19-C18	142.63522	177.91219
C17-C18-C20-C25	160.29872	166.95496	O16-C17-C18-C20	179.92739	-179.56154
C7-C11-C12-NI4	140.75331	179.49238	C8-C7-C11-C12	177.34999	178.80198
N10-C11-C12-O13	138.41786	169.16589	C21-C22-C23-CI26	179.28264	179.71435

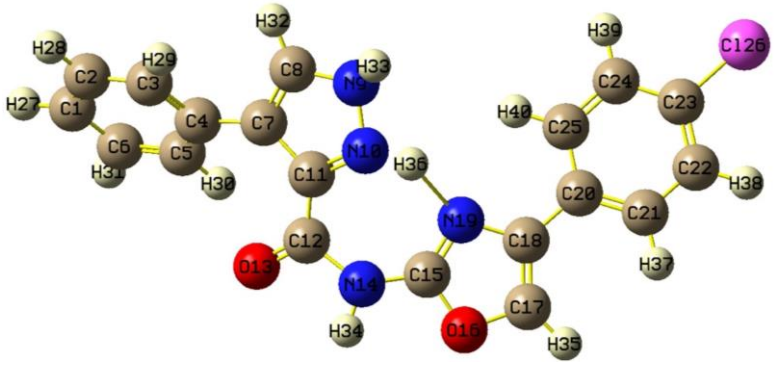

Figure 1. Optimized geometry representation of NOPC compound by PBEPBE method.

3.2. Mulliken atomic charges

The impact of SARS-CoV-2 on the global health system has necessitated the design of new antiviral agents and the understanding of their mechanisms of action [21, 24]. In this context, theoretical calculations and *in silico* analyses at the molecular level have become an important tool in the identification of potential inhibitors [25, 26]. Mulliken charge analysis, which is used for the detailed examination of the electronic structure, contributes to the elucidation of possible interaction sites with target proteins by determining the electron distribution within the molecule. In the present study, the electronic properties of the NOPC compound were optimized using the B3PW91 and PBEPBE functionals in combination with the 6-31G(d,p) basis set, followed by the calculation of Mulliken charge distributions. The results obtained in the Mulliken analysis have been given in Table 2. The results show that especially some nitrogen (N14, N19) and oxygen atoms on the molecule carry significant negative charges and these regions can serve as potential hydrogen bond acceptors. On the other hand, hydrogen atoms such as H33 attached to N9 carry more positive charges, which increases the potential of these regions to bind to protein receptors via electrostatic interactions. These active sites identified based on Mulliken charge distribution were then integrated into molecular docking analysis with SARS-CoV-2 core proteases (PDB ID: 6W75) and RNA-dependent RNA polymerase (RdRp; PDB ID: 7BV2). It has been observed that NOPC compound establishes strong hydrogen bonds and electrostatic interactions with critical amino acids such as ASN459, ARG349 and PHE396 in the enzyme PDB ID: 7BV2, especially through highly negatively charged nitrogen and

oxygen atoms. These interactions stabilize the binding conformation of the ligand and also reveal the molecular basis of its inhibitory effect. In addition, the fact that the charges carried by the carbon atoms vary between positive and negative values strengthens the possibility that these regions bind to the target protein by π-π stacking or van der Waals interactions. This electronic perspective provided by Mulliken charge analysis, combined with the docking results, indicates that NOPC compound may be a potential inhibitor against SARS-CoV-2.

The Mulliken atomic charge distribution in the NOPC (N-(4-(4-chlorophenyl)oxazol-2-yl)-4-phenyl-1*H*-pyrazole-3-carboxamide) compound is generally consistent with the literature trends observed in heteroaromatic and amide-containing molecules. Studies at the theoretical level, such as B3LYP/6-31G(d,p), have shown that heteroatoms (especially N and O) carry significant negative charges in their charge distribution and that carbon atoms can show both positive and negative values [27]. In NOPC, four nitrogen atoms (N9, N10, N14 and N19) carry significantly negative charges, and especially the N14 and N19 atoms belonging to the amide group showed values in the range of −0.55 to −0.61 in the calculations. This result supports DFT studies showing that nitrogen atoms generally have high charge density in pyrazole and similar N-containing heterocyclic systems. This trend has been frequently reported in the literature in heterocyclic molecules where heteroatoms carry high negative charges by Mulliken analysis [28].

Table 2. The NOPC molecule's theoretically determined Mulliken Atomic Charges.

ATOM	B3LYP	PBEPBE	ATOM	B3LYP	PBEPBE
C1	-0.081	-0.091	N9	-0.320	-0.342
C3	-0.119	-0.123	N10	-0.336	-0.461
C5	-0.105	-0.078	N14	-0.555	-0.611
C7	-0.061	-0.031	N19	-0.584	-0.591
C11	0.175	0.245	O13	-0.488	-0.496
C15	0.513	0.746	O16	-0.442	0.421
C17	0.121	0.055	H27	0.085	0.094
C20	0.098	0.070	H29	0.075	0.085
C22	-0.078	-0.088	H31	0.090	0.098
C24	-0.072	-0.084	H33	0.286	0.289
C25	-0.126	-0.120	H38	0.112	0.122
CI26	-0.021	0.004	H40	0.106	0.123

3.3. HOMO and LUMO analysis

The highest occupied molecular orbital (HOMO) and lowest unoccupied molecular orbital (LUMO) energy Moreover, DFT investigations of various pyrazole-containing compounds have demonstrated that HOMO and LUMO energy levels directly influence electron donor–acceptor behavior. These levels represent essential parameters for interpreting molecular electronic properties and provide valuable insight into chemical reactivity, stability, and interactions with biological targets [29, 30]. HOMO reflects the tendency of the molecule to donate electrons, while LUMO represents the ability to accept electrons [31, 32]. The energy gap (ΔE) between these orbitals influences the molecule's chemical stability and reactivity, as well as its potential interactions with biological targets. In this work, quantum chemical analyses were carried out on the NOPC molecule using density functional theory (DFT). The compound was evaluated for its potential inhibitory interactions with the SARS-CoV-2 main protease enzymes (PDB IDs: 6W75 and 7BV2). The HOMO and LUMO parameters obtained from two different computational methods are listed in Table 3. Visual representations of the HOMO and LUMO orbitals of NOPC are provided in Figures 2 and 3. These quantum chemical parameters were determined using Equations (1–6). For the optimized structure with the 6-31G(d,p) basis set, the HOMO–LUMO energy gap was found to be 1.531 eV using B3LYP and 1.969 eV using PBEPBE. This narrow band gap indicates that the molecule has high chemical reactivity and the capacity to interact effectively with possible biological targets. NOPC showed strong binding with critical residues (ASN459, ARG349 and PHE396) located in the active site of the protease via hydrogen bonds and hydrophobic interactions. Furthermore, the overlap of HOMO and LUMO distribution with π-systems and electrophilic/nucleophilic regions in the ligand structure supported the interactions with the active site, which was consistent with the docking results. Electrophilicity indices (B3LYP: 3.2791; PBEPBE: 2.5162) also reveal that the molecule has a high reactivity potential and can effectively bind to biological targets. These results show that NOPC molecule can be considered as a potential inhibitor against SARS-CoV-2 and HOMO–LUMO analyses are an important tool in the prediction of biological activity.

The HOMO–LUMO energy values of NOPC (B3LYP: ΔE= 1.53 eV; PBEPBE: ΔE=1.97 eV) obtained in this study show significant differences when compared with DFT-based approaches commonly used in evaluating the electronic structures of heterocyclic systems. Studies of pyrazolo[1,5-c]pyrimidin-7(1*H*)-one derivatives at the DFT/B3LYP level reported in the literature show that HOMO–LUMO gaps are relatively higher, and this is associated with chemical stability, revealing a higher potential for electronic reactivity compared to the lower energy gap of NOPC [33]. Similarly, HOMO–LUMO analyses of the molecular structure of 3-(4-chlorophenyl)-5-aryl-1*H*-pyrazol-1-yl methanol derivatives have been reported with larger energy gaps reflecting intermolecular charge transfer tendencies, indicating that ΔE strongly reflects molecular stability in such pi-conjugated heterocyclic systems [34]. Moreover, DFT

investigations of various pyrazole-containing compounds have demonstrated that HOMO and LUMO energy levels directly influence electron donor–acceptor behavior. These levels represent essential parameters for interpreting molecular electronic properties and provide valuable insight into chemical reactivity, stability, and interactions with biological targets.molecule, with smaller energy gaps associated with higher reactivity and potential biological interactions. It is emphasized that [35].

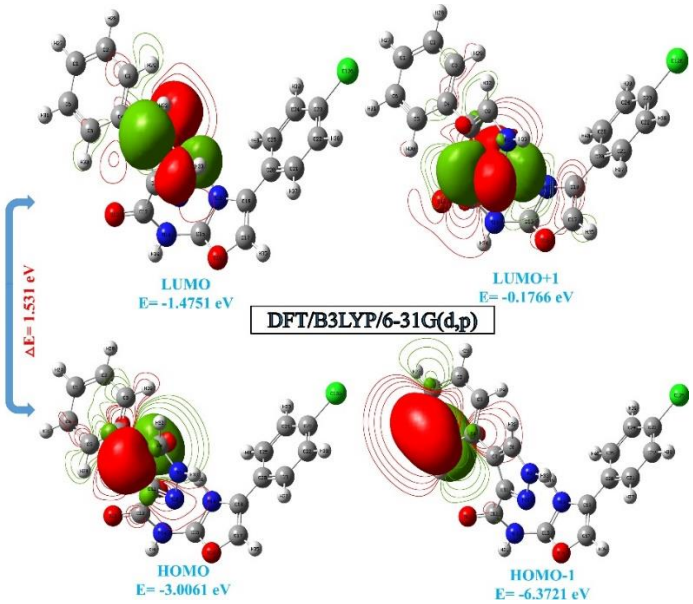

Figure 2. Frontier orbitals of NOPC calculated at the B3LYP/6-31G(d,p) level.

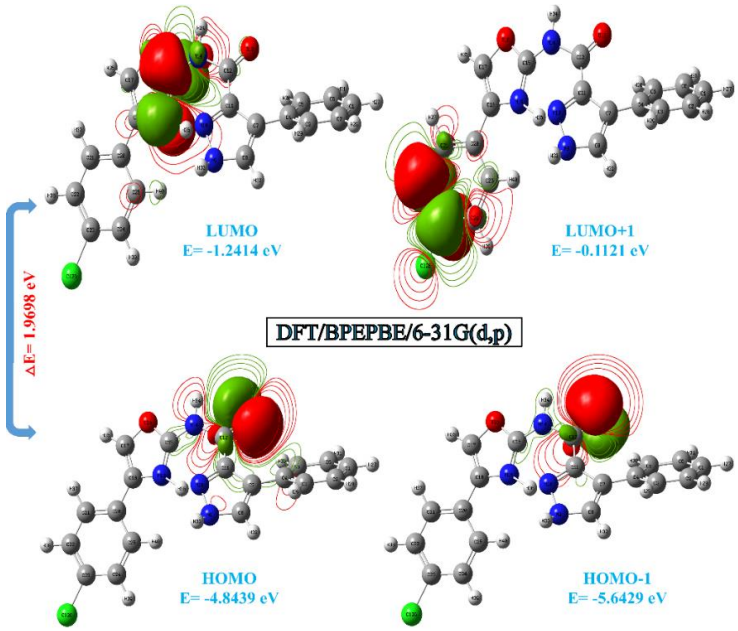

Figure 3. Frontier orbitals of NOPC calculated at the PBEPBE/6-31G(d,p) level.

$$\Delta E = |EHOMO - ELUMO| \quad (1)$$

$$\eta = (I - A)/2 \quad (2)$$

$$s = I/2\eta \quad (3)$$

$$\mu = \frac{I+A}{2} \quad (4)$$

$$\chi = (1 + A) \quad (5)$$

$$\omega = \mu^2/2\eta \quad (6)$$

Table 3. HOMO–LUMO characteristics of NOPC computed by B3LYP and PBEPBE methods.

	E_{HOMO}	E_{LUMO}	ΔE	I	A	η	s	μ	χ	ω
B3LYP	-3.0061	-1.4751	1.531	3.0061	1.4751	0.7655	1.9635	2.2406	1.2375	3.2791
PBEPBE	-3.2112	-1.2414	1.969	3.2112	1.2414	0.9849	1.6302	2.2263	1.1207	2.5162

ΔE→Energy Gap, I→Ionization Potential($-E_{HOMO}$), A→Electron Affinity($-E_{LUMO}$), η→Chemical hardness, s→Chemical softness, μ→Chemical Potential, χ→Electronegativity, ω→Electrophilicity index

3.4. Molecular electrostatic potential (MEP)

MEP maps are used as a very effective tool in determining the potential reactive sites of a molecule by visualizing the spatial distribution of the electrostatic potential around it [36-38]. In this study, the MEP map of the NOPC molecule was obtained using the 6-31G(d,p) basis set with B3LYP and PBEPBE functionals based on density functional theory (DFT). The MEP map of the NOPC molecule calculated by the gas phase study methods has been shown in Figure 4. As a result of the calculations, the potential values for the B3LYP method varied between -7.138 eV and +7.138 eV, while this range was found to be -6.199 eV and +6.199 eV for the PBEPBE method. These values reveal that the distribution of electrostatic potential around the molecule varies depending on the methods. In the obtained MEP maps, color coding represents potential differences. The regions shown in red on the map have high electron density and are generally concentrated around electronegative atoms (e.g. oxygen and nitrogen). These regions show high affinity for electrophilic agents and are evaluated as possible reaction centers. Blue regions indicate electron-poor zones, usually associated with hydrogen atoms or positively charged centers. MEP mapping provides crucial information for identifying likely reactive regions in the NOPC molecule, which were subsequently considered in docking simulations against SARS-CoV-2. The significant negative potential around the carbonyl oxygen implies that this area can engage in strong electrostatic contacts with electrophilic amino acid residues of the viral protease. Similarly, the positive potential areas detected around the hydrogen atoms attached to the nitrogen group suggest that it can interact with nucleophilic viral target regions via hydrogen bonding. Molecular docking analyses performed in line with these electrostatic properties revealed that the NOPC molecule can bind to the active site of the SARS-CoV-2 main protease (6W75 and 7BV2 proteins) with high affinity, and especially the carbonyl oxygen and nitrogen group interactions played a decisive role in binding stability. These findings reveal that MEP analysis provides important contributions not only in the identification of reactive regions but also in the prediction of ligand-target interactions. The calculated MEP values for the NOPC compound ranged from −7.138 to +7.138 eV and −6.199 to +6.199 eV at the B3LYP/6-31G(d,p) and PBEPBE/6-31G(d,p) levels, respectively, and these ranges are consistent with similar heterocyclic carboxamide and pyrazole derivatives in the literature in terms of electron density distribution across MEP surfaces. For example, in a DFT study on heterocyclic aromatic compounds such as 4-phenylpyrimidine, MEP analysis showed that the determination of negative potential regions on the molecular surface is reactivity determinant [39]. Furthermore, it has been reported that the MEP distribution in heteroatom-containing molecules clearly reveals electron-rich (suitable for electrophilic attack) and electron-poor (suitable for nucleophilic interactions) regions; These studies emphasize that negative potential regions around the carbonyl oxygen are critical for reactive interactions [40]. The literature also reports that MEP analyses performed on similar heterocyclic structures have proven to be an effective tool in evaluating intermolecular hydrogen bonding and electrostatic interactions [41]. These findings support the idea that the electrostatic potential distribution of NOPCs can be used to assess reactivity and bonding properties.

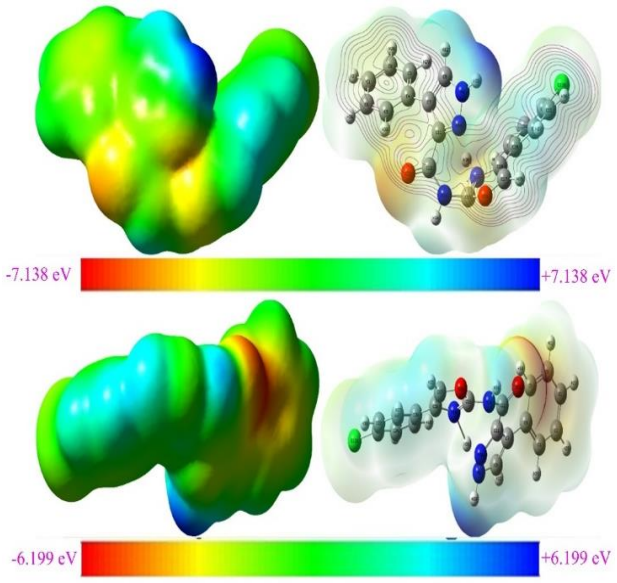

Figure 4. MEP map of the NOPC molecule calculated by B3LYP and PBEPBE methods.

3.5. Non-linear optical properties (NLO)

Nowadays, the design of molecules with nonlinear optical (NLO) properties stands out as an important research area in optical data storage systems and modern communication Technologies [42, 43]. In this context, dipolar molecules, especially those containing electron donor and electron acceptor groups, are

among the most investigated structures in the development of NLO properties. Some standard compounds are used as references for the understanding and comparative evaluation of NLO properties at the molecular level [44]. Urea, one of these compounds, is widely accepted as a reference point in the evaluation of nonlinear optical properties in theoretical studies [45]. The nonlinear optical characteristics of urea were theoretically evaluated in this work, and the derived values were offered as a benchmark for subsequent studies. Table 4 shows the dipole moment (μ), polarizability (α), and first hyperpolarizability (β) of NOPC obtained through two distinct computational approaches. When these data are evaluated with the comparisons made with urea, it is observed that the relevant parameters of NOPC in the gas phase are approximately eight times higher. This significant difference reveals that NOPC has a great potential in terms of nonlinear optical properties. These findings indicate that NOPC is an important candidate especially in the field of optoelectronic applications and nonlinear optical materials. Nonlinear optical (NLO) properties play an important role in the study of changes in the electronic structures of molecules, especially in biological systems. NLO active compounds can provide a strong polarization response due to the asymmetric properties in their electron density distributions, which makes them valuable for biosensor applications and drug design. In this context, the combined use of both NLO properties and molecular docking analyses in the determination of potential inhibitors against the SARS-CoV-2 virus provides a comprehensive evaluation of both optoelectronic and biological activities of molecules. Studies have shown that some compounds with high hyperpolarizability exhibit high binding affinity to the target proteins of SARS-CoV-2. This approach provides a multidisciplinary perspective in the development of new antiviral agents, enabling the joint analysis of both optical properties at the molecular level and interactions with biological targets.

Many studies have investigated the NLO properties of heterocyclic and pi-conjugated organic systems using B3LYP and similar DFT methods. For example, a study on 1,2,4-triazole and phenylpropanamide derivatives showed that the total β values calculated by femto DFT were in the order of 6.3×10^{-30} esu, indicating that these compounds are promising for optoelectronic applications; It has been stated that this increased hyperpolarizability value is related to the electron migration effect in the molecular structure and the contribution of bound heteroatoms [46]. The fact that the β values obtained at the B3LYP and PBEPBE levels in your calculations for the NOPC molecule are in the range of 1.55×10^{-30} -1.58×10^{-30} esu shows that the NLO efficiency of heterocyclic core organic compounds is of the same order of magnitude compared to similar systems in the literature. These results reveal that heterocyclic pi-systems, particularly those with N-a, can achieve significant hyperpolarizability through charge concentration and molecular asymmetry 3 [46]. On the other hand, some pi-conjugated systems reported in the literature show much higher β values (around 2.9×10^{-29} esu) for example, 1,3,4-oxadiazole derivatives; it is stated that in such systems, the strong electron donor-acceptor interaction and the larger conjugation structure significantly increase hyperpolarizability, which may be the reason for the higher β values compared to NOPC [47].

Table 4. NLO parameters of the NOPC molecule calculated using B3LYP and PBEPBE methods.

Parameters	B3LYP	PBEPBE	Parameters	B3LYP	PBEPBE
μ_x	5.7484	5.2424	β_{XXX}	33.4129	32.6351
μ_y	-1.4583	-1.5570	β_{YYY}	11.4750	9.0032
μ_z	-0.8744	-0.8993	β_{ZZZ}	-17.9272	-17.4776
$\mu_{(D)}$	5.9946	5.5422	β_{XYY}	37.0192	33.7689
αxx	-147.9027	-147.7385	β_{XXY}	-100.5969	-96.1515
α_{YY}	-156.3746	-154.4782	β_{XXZ}	60.0632	62.3132
α zz	-155.8632	-154.8301	β_{XZZ}	-11.8166	-14.7312
α_{XY}	-8.1752	-7.2873	β_{YZZ}	-5.2132	33.7689
α_{XZ}	-7.6218	-7.5954	β_{YYZ}	-22.2425	-21.4024
α_{YZ}	6.7476	6.3255	β_{XYZ}	-15.6334	-13.5984
α(au)	-133.1339	-137.3467	β(esu)	$1.55\text{x}10^{-30}$	$1.58\text{x}10^{-30}$

Urea (Reference)= $\mu_{(D)}$ = 1.3197, β(esu) = $0.1947\text{x}10^{-3}$

3.6. NBO analysis

NBO analysis is a powerful method that allows detailed investigation of intramolecular and intermolecular bonding and bond interactions [48]. It is also an important tool for understanding charge transfers and conjugative interactions occurring in molecular systems [49]. NBO analysis was carried out for the NOPC molecule optimized using the PBEPBE/6-31G(d,p) method. Table 5 presents the results, including intramolecular delocalization interactions, hybridization details, and electron

density distributions. Analysis results, the second-order stabilization energy that defines the interactions between electron donor and acceptor orbitals is usually calculated as follows:

$$E^{(2)} = -n_i \cdot \frac{(Fij)^2}{\mathcal{E}_j - \mathcal{E}i} \quad (7)$$

- n_i : Number of electrons in donor orbital
- Fij : Fock matrix element between donor and acceptor orbitals
- $\mathcal{E}_j - \mathcal{E}i$: Acceptor and donor orbital energies

The magnitude of these values indicates the intensity of conjugative interactions between the relevant orbitals and the degree of charge transfer within the system. The highest interaction was determined with a value of 19.98 kcal/mol calculated for the π*(C22–C23) → π*(C20–C21) transition. This situation reveals the existence of a strong π-π* conjugation between the orbitals in question. On the other hand, the lowest interaction was observed with 0.50 kcal/mol for the σ(C15–N19) → σ*(C18–C20) transition, indicating that this interaction is quite weak. The interaction of the chosen compound with SARS-CoV-2 main proteases (6W75 and 7BV2) was explored through molecular docking and NBO analysis. Molecular docking demonstrated that the compound binds strongly to both enzymes, and NBO analysis was used to assess electron density redistribution, conjugation effects, and hybridization patterns within the ligand–protein complex. In the NBO analysis, the second-order stabilization energy (E(2)) values, especially between the donor (electron donating) and acceptor (electron receiving) orbitals, quantitatively revealed the electronic interactions of the compound with the amino acid residues in the binding site. The high E(2) values obtained indicate that the compound establishes strong π-π or σ-σ conjugative interactions with some amino acids in the active site and thus forms stable complexes with protease enzymes. These findings support that the compound could be a potential inhibitor candidate targeting the main proteases of SARS-CoV-2.

NBO (Natural Bond Orbital) analysis shows that the π-system is significantly delocalized in the NOPC compound and contributes significantly to the overall stability of the molecule. In particular, the C22–C23 π→C20–C21 π* (E(2)=19.98 kcal/mol) and C22–C23 π→C24–C25 π* (E(2)=17.73 kcal/mol) transitions are consistent with the strong π→π* interactions observed in aromatic/conjugated systems. Similarly, in pyrazol-oxazole and similar heteroaromatic systems reported in the literature, π→π* stabilization energies are typically reported in the range of 15–22 kcal/mol, which supports the fact that NOPC exhibits a high degree of conjugation and resonance stabilization [50, 51]. Furthermore, the π*→π* interactions observed in NOPC (C7–C8 π* → C3–C4 π*; E(2)=10.28 kcal/mol) parallel the significant antibonding-antibonding interactions reported in similar heteroaromatic molecules [52]. The σ→σ* and σ→π* transitions (N14–H34 σ→C15–N19 σ*, E(2)=0.80 kcal/mol; O16–C17 σ→N14–C15 σ*, E(2)=0.57 kcal/mol) correspond to the typical hyperconjugation level seen in amide/heteroatomic systems in the literature and partially contribute to the bond stability of the molecule [53].

Table 5. Selected NBO results of NOPC molecule calculated using PBEPBE/6-31G(d,p) basis sets.

NBO(i)	Type	Occupancies	NBO(j)	Type	Occupancies	E(2)[a] (Kcal/mol)	E (j)-E(i)[b] (Kcal/mol)	F (i, j)[c] (Kcal/mol)
C1-C2	π	0.83071	C3-C4	π*	0.19200	1.76	144.33	32.65
C1- C2	π	0.83071	C5-C6	π*	0.15449	1.69	144.33	32.65
C3-C4	π	0.82402	C1-C2	π*	0.17283	1.81	144.33	33.28
C3-C4	π	0.82402	C5-C6	π*	0.15449	1.70	144.33	32.65
C3-C4	π	0.82402	C7-C8	π*	0.14840	1.36	131.78	28.24
C5-C6	π	0.82886	C1-C2	π*	0.17283	1.84	137.95	33.28
C5-C6	π	0.82886	C3-C4	π*	0.19200	1.76	144.33	32.65
C11-C12	π	0.93085	C7-C8	π*	0.14840	1.70	150.60	34.51
N14-H34	σ	0.98692	C15-N19	σ*	0.23844	0.80	659.88	47.06
C15-N19	σ	0.99280	C18-C20	σ*	0.01657	0.50	771.84	40.79
C15-N19	π	0.93968	C17-C18	π*	0.14660	1.81	181.88	38.90
O16-C17	σ	0.99200	N14-C15	σ*	0.00842	0.57	765.81	42.71
C18-N19	σ	0.98301	N14-C15	σ*	0.00842	1.12	696.03	57.09
C20-C21	π	0.81369	C17-C18	π*	0.14660	1.74	137.95	32.65
C20-C21	π	0.81369	C22-C23	π*	0.20501	1.98	131.78	33.87
C17-H30	π	0.98886	C16-C21	π*	0.01559	0.76	577.91	42.71
C20-C21	π	0.81369	C24-C25	π*	0.15758	1.75	144.33	32.65
C22-C23	π	0.83301	C20-C21	π*	0.19544	1.60	150.60	32.65
C22-C23	π	0.83301	C24-C25	π*	0.15758	1.68	150.60	33.28
C24-C25	π	0.83659	C20-C21	π*	0.19544	1.70	144.33	32.65
C24-C25	π	0.83659	C22-C23	π*	0.20501	1.79	137.95	32.65

C7-C8	π*	0.14840	C3-C4	π*	0.19200	10.28	6.28	33.87
C11-C12	π*	0.26219	C7-C8	π*	0.14840	10.04	12.55	34.51
C15-N19	π*	0.23844	C17-C18	π*	0.14660	4.34	18.83	31.38
C22-C23	π*	0.20501	C20-C21	π*	0.19544	19.98	12.55	45.18
C22-C23	π*	0.20501	C24-C25	π*	0.15758	17.73	6.28	42.71

3.7. Molecular docking studies

In this study, SARS-CoV-2 was selected as the biological target due to its continued global impact and the urgent need for novel antiviral agents. Although vaccines have significantly reduced the severity of COVID-19, the emergence of new variants and breakthrough infections highlights the necessity of developing additional therapeutic strategies. Among the viral proteins, the main protease (Mpro) and RNA-dependent RNA polymerase (RdRp) were chosen because they are essential for viral replication and exhibit high conservation across SARS-CoV-2 variants, making them promising targets for broad-spectrum inhibitors. Mpro mediates the proteolytic processing of viral polyproteins into functional non-structural proteins, and its inhibition effectively blocks viral maturation. RdRp is responsible for viral RNA synthesis and has no close human homolog, which increases the likelihood of selective inhibition. The selected PDB structures, 6W75 and 7BV2 (RdRp), were used because they provide high-resolution, experimentally validated conformations with clearly defined active sites and cofactor binding regions, allowing reliable docking simulations. Although other SARS-CoV-2 proteins such as the spike protein, papain-like protease (PLpro), helicase (nsp13), and exoribonuclease (nsp14) are also relevant, the current work focuses on replication-related enzymes due to their established druggability and extensive use in antiviral drug discovery.

The 2D structure of the NOPC ligand was plotted using ChemDraw and saved in MDL SD format (SDF). The ligand geometry was not subjected to DFT optimization; the 3D structure obtained from the SDF file was used directly for docking studies. Target proteins (PDB ID: 6W75; PDB ID: 7BV2) were downloaded from the Protein Data Bank. Protein preparation (removal of water molecules, addition of hydrogen, and optimization of protonation states) was performed using Schrödinger Maestro (version 11.8) software. The binding site for docking was defined using the Receptor Grid Generation module in Maestro, based on the active site containing the co-crystallized ligand in the crystal structure. Grid dimensions were adjusted to completely encompass the active site amino acids and were determined as 20×20×20 Å for Mpro and RdRp. Docking simulations were performed using the Glide module with these grid parameters.

Structure-based drug design is a rational drug discovery approach that aims to develop inhibitory or agonist compounds with high specificity by utilizing three-dimensional structural information of the target protein. In this context, molecular docking methods are widely used to predict possible binding conformations and binding affinities of small molecules with biological targets [54]. These methods, based on computational modeling techniques, provide significant advantages in terms of both cost and time compared to traditional high-throughput screening methods [55]. In addition, they provide valuable insights in terms of structural optimization and biological activity prediction of candidate molecules by allowing atomic-level analysis of ligand-protein interactions [56]. Therefore, molecular docking-based virtual screening approaches are among the indispensable components of early-stage drug discovery processes. The impact of the COVID-19 pandemic on global health has made the development of effective antiviral agents against the SARS-CoV-2 virus a priority area of research [57]. In this context, molecular docking studies conducted within the framework of structure-based drug design approaches offer the opportunity to evaluate the interactions of potential inhibitors with viral target proteins at the molecular level [58]. In this study, the potential binding affinity of the NOPC molecule, a pyrazole derivative, with the main protease (PDB ID: 6W75) and RNA-dependent RNA polymerase (PDB ID: 7BV2), one of the critical enzymes of SARS-CoV-2, was investigated. In this study, Discovery Studio Visualizer (version 2016) [59] software was used to visualize protein-ligand interactions. As a result of molecular docking analyses, it was determined that the ligands bind to the active sites of target proteins with high affinity; it was observed that the amino acid residues in these binding sites have different physicochemical properties (Figure 5). In line with the docking results, the most suitable binding conformations were obtained and these positions have been visually presented in Figure 6 and Figure 7. In particular, the interactions of the NOPC compound with the target proteins were evaluated in detail and the critical amino acid residues in the binding site and the types of interactions between them have been shown in Table 6. Binding energy calculations revealed that NOPC obtained docking scores of −7.70 kcal/mol for 6W75 and −8.40 kcal/mol for 7BV2 (Table 6), indicating strong and specific binding to these proteases. The simulations were performed with Schrödinger Maestro (version 11.8) [15] software, The results indicated that NOPC achieved high binding scores with both of the target proteins. Especially the

high binding affinity obtained in the interaction with RdRp target indicates that this compound may be a strong candidate for the inhibition of viral replication mechanism. Interaction analyses performed using Discovery Studio software revealed that numerous hydrogen bonds, π–π stacking and hydrophobic interactions were formed between the ligand and the target protein. These interactions support the conformationally stable placement of the ligand in the binding site and strengthen its inhibitory potential. These results indicate that NOPC may be regarded as a promising multi-target antiviral agent against SARS-CoV-2. Moreover, the compound's pharmacological effects and safety profile should be evaluated in detail using comprehensive *in vitro* and in vivo experiments. The docking protocol was validated by re-docking the co-crystallized ligands into the active sites of the target proteins, and the root-mean-square deviation (RMSD) values were calculated using the MOE program [16]. As shown in Table 6, the RMSD values obtained for the re-docked poses of NOPC with 6W75 and 7BV2 were 1.5584 Å and 1.4212 Å, respectively. These RMSD values are well below the widely accepted threshold of 2.0 Å, indicating a strong agreement between the experimentally observed and predicted binding conformations. Consequently, the docking protocol can be considered reliable, and the predicted binding modes of NOPC within the active sites of both target proteins are deemed accurate.

Table 6. Molecular docking interactions scores with PDBID: 6W75, PDBID: 7BV2 enzymes of NOPC compound.

NOPC Compound	PDB: 6W75	PDB: 7BV2
Docking Score	-7.70	-8.40
RMSD Values	1.5584	1.4212

Table 7. The interaction parameters between NOPC compound and 6W75, 7BV2 enzyms.

	6W75 Enzym			7BV2 Enzym		
Important Interactions	Full Name	Type	Bond Length(Å)	Full Name	Type	Bond Length(Å)
Van der Waals	MET6929	Methionine	-	THR394	Threonine	-
	ASN6899	Asparagine	-	CYS395	Cysteine	-
	SER6872	Serine	-	SER318	Serine	-
	GLY6869	Glycine	-	GLU350	GlutamicAcid	-
	GLU7001	GlutamicAcid	-	PRO677	Proline	-
	THR6970	Threonin		ASN28	Asparagine	
Conventional Hydrogen Bond	ASN6841	Asparagine	5.39	ASN459	Asparagine	3.11
	LYS6968	Lysine	5.74	ASP464	Arginine	5.94
	LYS6844	Lysine	5.98	ARG574		
Pi-Anion	ASP6897	AsparticAcid	7.07	-	-	-
	ASP6928	AsparticAcid	5.96			
Pi-Sigma	-	-	-	PRO677	Proline	4.12
Pi-Cation	LYS6935	Lysine	7.84	ARG349	Arginine	6.98
Amide-Pi stacked	-	-	-	LEU460	Leucine	4.71
Alkyl	LEU6998	Leucine	4.36	-	-	-
Pi-Alkyl	-	-	-	VAL315	Valine	6.10
				PRO323	Proline	5.01
Carbon Hydrogen Bond	GLY6869	Glycine	5.20	-	-	-
Pİ-Pi Stacked	-	-	-	PHE396	Phenylalanine	5.18
Pi-Donor Hydrogen Bond	-	-	-	-	-	-
Pİ-Pi T-Shaped	TYR6930	Tyrosine	4.36	-	-	-

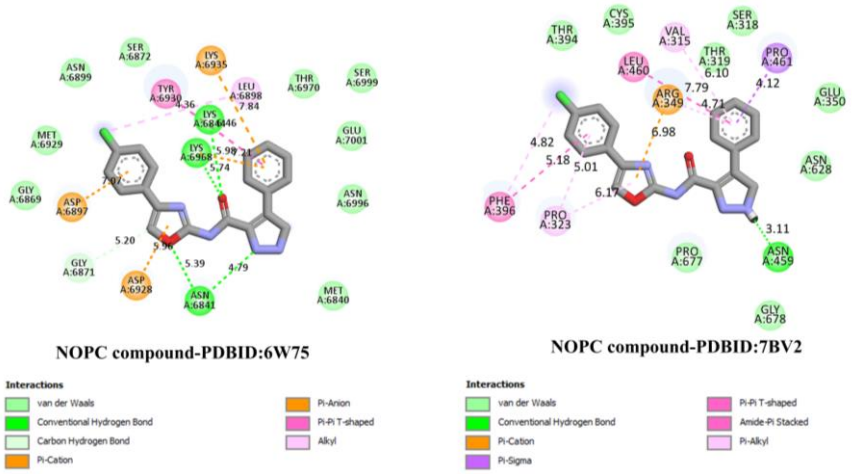

Figure 5. 2D Mode view of NOPC Compound and PDBID: 6W75, PDBID: 7BV2 enzyms.

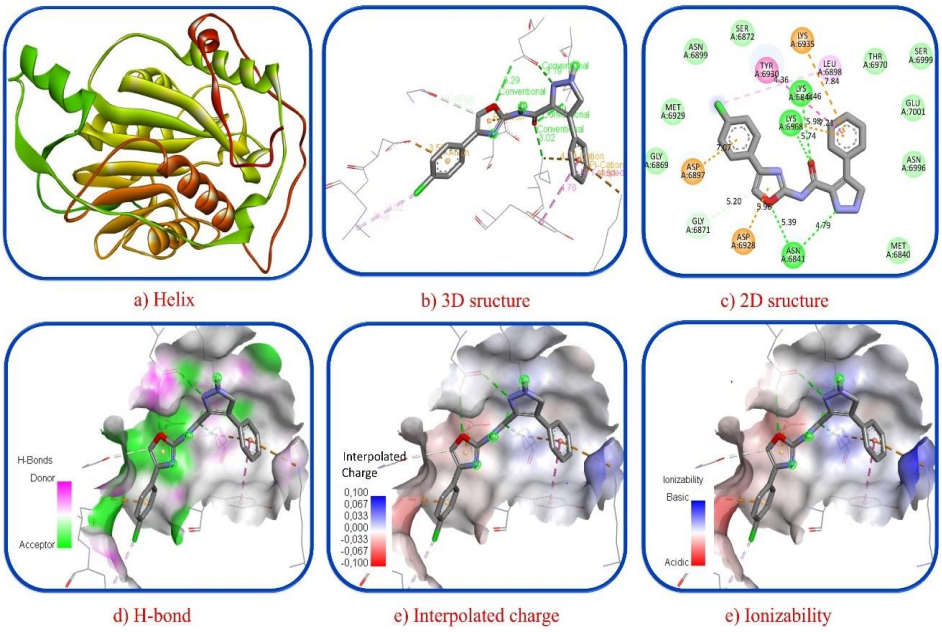

Figure 6. Molecular docking visual results of NOPC compound with 6W75 enzyme.

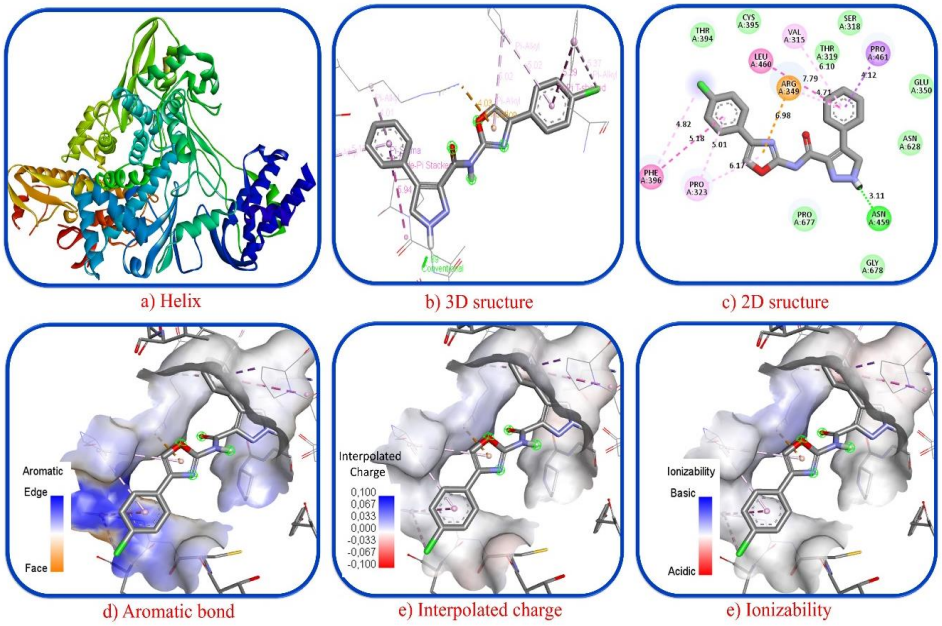

Figure 7. Molecular docking visual results of NOPC compound with 7BV2 enzyme

3.8. ADME Analysis

Nowadays, in drug discovery processes, early prediction of pharmacokinetic and pharmacodynamic properties of candidate compounds is of great importance in terms of reducing drug development costs and accelerating the process [60]. In this context, *in silico* methods enable the pre-evaluation of ADME parameters covering absorption, distribution, metabolism and excretion processes, allowing results to be obtained in a shorter time, at lower cost and with higher efficiency compared to experimental studies [61]. In this study, NOPC compound was analyzed *in silico* using ADMETlab 2.0 platform (https://admetmesh.scbdd.com/). Table 8 shows the calculated molecular properties of Lipinski's rule of five determined using ADMETlab 2.0 online tool. The compound fully complied with Lipinski's Rule of Five, revealing that it is a potential drug candidate with oral bioavailability. It offers a favorable pharmacokinetic profile with its properties such as high intestinal absorption (HIA), ability to cross the blood-brain barrier (BBB permeability), strong binding to plasma proteins (95.7%) and the ability to inhibit liver enzymes such as CYP2D6 and CYP3A4. In addition, the half-life (T1/2) of the compound along with its renal and hepatic clearance values provides information about its persistence in systemic circulation and duration of activity; which plays a critical role in determining dosing intervals. The aforementioned pharmacokinetic and physicochemical data support the evaluation of NOPC as a lead drug candidate; and form the scientific basis for carrying this compound to *in vitro* and *in vivo* studies to be conducted at later stages. Therefore, such *in silico* analyses stand out as a powerful pre-screening tool in terms of rational molecule design and candidate selection in the drug development process. When the *in silico* ADME profile analysis results of the compound are evaluated together with the docking results, the NOPC compound stands out as a promising antiviral candidate with both its target-specific binding potential and appropriate ADME profile against SARS-CoV-2. The color regions and physicochemical parameter maps of the NOPC compound have been given in Figure 8.

Table 8. NOPC molecule's physicochemical and lipophilicity.

Property	NOPC	Comment
Molecular Weight	364.07	Molecular Weight< 500
nHA	6	Hydrogen bond acceptors< 12
nHD	2	Hydrogen bond donors< 7
logP	4.302	Log of the octanol/water partition coefficien: 0-5
TPSA	83.81	Topological Polar Surface Area:0-140
HIA	0.00	Category 1: HIA+(HIA < 30%); Category 0: HIA-(HIA >= 30%); The output value is the probability of being HIA+
BBB	0.957	The output value is the probability of being BBB+
CYP2D6	0.00	Category 1: Inhibitor; Category 0: Non-inhibitor;

CYP3A4	0.005	The output value is the probability of being inhibitor. Category 1: Inhibitor; Category 0: Non-inhibitor; The output value is the probability of being inhibitor.
$T_{1/2}$	0.826	The unit of predicted T1/2 is hours. ultra-short half-life drugs: 1/2 < 1 hour; short half-life drugs: T1/2 between 1-4 hours; intermediate short half-life drugs: T1/2 between 4-8 hours; long half-life drugs: T1/2 > 8 hours.

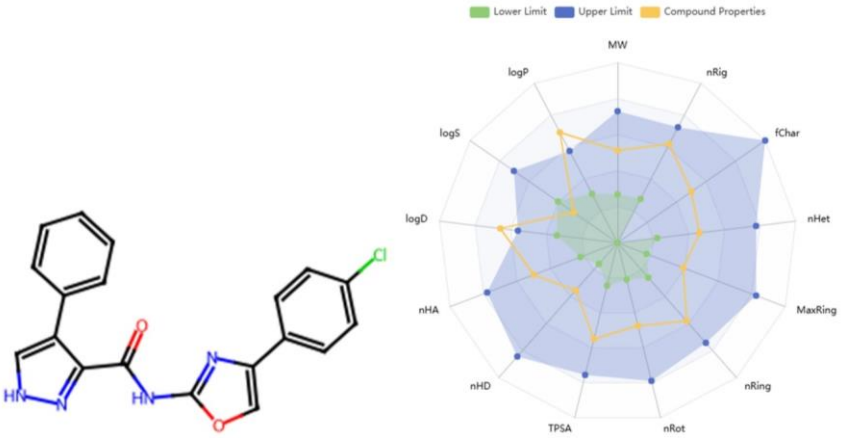

Figure 8. Color regions and physicochemical parameters of NOPC molecule.

4. Conclusions

In this study, the molecule NOPC compound was investigated comprehensively for the first time using multidimensional theoretical calculations and molecular modeling approaches. Structural and electronic data obtained with DFT optimizations (B3LYP/6-31G(d,p) and PBEPBE/6-31G(d,p)) demonstrated high agreement between the two methods, confirming the reliability of the calculations. The HOMO–LUMO energy gap and the obtained chemical reactivity parameters showed that NOPC has high chemical stability and controlled reactivity. MEP analysis identified potential interaction sites on the molecule, revealing suitable binding sites for hydrogen bonding and electrostatic interactions. Pharmacokinetic evaluations (ADMETlab 2.0) showed that NOPC satisfies Lipinski's Five Rules and has a favorable profile in terms of oral bioavailability. These results support the molecule's potential to enter systemic circulation and be evaluated among drug candidates. Molecular docking studies revealed that NOPC exhibited binding affinities of −7.70 kcal/mol and −8.40 kcal/mol to SARS-CoV-2 major protease (PDB ID: 6W75) and RNA-dependent RNA polymerase (PDB ID: 7BV2), respectively. These findings strongly support NOPC's potential as a dual-target inhibitor against two critical enzymes of the virus. Overall, the findings demonstrate that NOPC is both chemically stable and amenable to interaction with biological targets; it stands out as a novel starting compound that can be evaluated, particularly in antiviral drug development studies targeting SARS-CoV-2. Further studies are recommended to confirm this potential in more detail with molecular dynamics simulations and *in vitro/in vivo* biological tests.

Conflict of interests

The authors declare no conflict of interest.

Declaration of Ethical Code

In this study, we undertake that all the rules required to be followed within the scope of the "Higher Education Institutions Scientific Research and Publication Ethics Directive" are complied with, and that none of the actions stated under the heading "Actions Against Scientific Research and Publication Ethics" are not carried out.

References

[1] Oliveira, B. G., Araújo, R. C. M. U., Carvalho, A. B., Ramos, M. N. 2009. *The molecular properties of heterocyclic and homocyclic hydrogen-bonded complexes evaluated by DFT calculations and AIM densities.* Journal of Molecular Modeling, 15(2), 123-131.

[2] Qadr, H. M., Mamand, D. M. 2021. *Molecular Structure and Density Functional Theory Investigation Corrosion Inhibitors of Some Oxadiazoles.* Journal of Bio- and Tribo-Corrosion, 7(4), 140.

[3] Azeem, M., Hanif, M., Mahmood, K., Ameer, N., Chughtai, F. R. S., Abid, U. 2023. *An insight into anticancer, antioxidant, antimicrobial, antidiabetic*

and anti-inflammatory effects of quercetin: a review. Polymer Bulletin, 80(1), 241-262.

[4] Davidova, S., Galabov, A. S., Satchanska, G. 2024. *Antibacterial, Antifungal, Antiviral Activity, and Mechanisms of Action of Plant Polyphenols.* Microorganisms, 12(12), 2502.

[5] Kakkar, S., Tahlan, S., Lim, S. M., Ramasamy, K., Mani, V., Shah, S. A. A., Narasimhan, B. 2018. *Benzoxazole derivatives: design, synthesis and biological evaluation.* Chemistry Central Journal, 12(1), 92.

[6] Sheena Mary, Y., Shyma Mary, Y., Temiz-Arpaci, O., Yadav, R., Celik, I. 2021. *DFT, docking, MD simulation, and vibrational spectra with SERS analysis of a benzoxazole derivative: an anti-cancerous drug.* Chemical Papers, 75(8), 4269-4284.

[7] Erol, M., Çelik, İ., Uzunhisarcıklı, E., İnce, U. 2022. *Virtual Screening And Molecular Docking Analysis On Three Sars-Cov-2 Drug Targets By Multiple Computational Approach.* Journal of Faculty of Pharmacy of Ankara University, 46(2), 376-392.

[8] Salzberger, B., Buder, F., Lampl, B., Ehrenstein, B., Hitzenbichler, F., Holzmann, T., Schmidt, B., Hanses, F. 2021. *Epidemiology of SARS-CoV-2.* Infection, 49(2), 233-239.

[9] Nuha, D., Evren, A. E., Çiyanci, Z. Ş., Temel, H. E., Akalin Çiftçi, G., Yurttaş, L. 2022. *Synthesis, density functional theory calculation, molecular docking studies, and evaluation of novel 5-nitrothiophene derivatives for anticancer activity.* Archiv der Pharmazie, 355(9), 2200105.

[10] Al-Wahaibi, L. H., Mostafa, A., Mostafa, Y. A., Abou-Ghadir, O. F., Abdelazeem, A. H., Gouda, A. M., Kutkat, O., Abo Shama, N. M., Shehata, M., Gomaa, H. A. M., Abdelrahman, M. H., Mohamed, F. A. M., Gu, X., Ali, M. A., Trembleau, L., Youssif, B. G. M. 2021. *Discovery of novel oxazole-based macrocycles as anti-coronaviral agents targeting SARS-CoV-2 main protease.* Bioorg Chem, 116(105363.

[11] Morsy, A. R., Mahmoud, S. H., Abou Shama, N. M., Arafa, W., Yousef, G. A., Khalil, A. A., Ramadan, S. K. 2024. *Antiviral activity of pyrazole derivatives bearing a hydroxyquinoline scaffold against SARS-CoV-2, HCoV-229E, MERS-CoV, and IBV propagation.* RSC advances, 14(38), 27935-27947.

[12] Nazir, M. S., Ahmad, M., Aslam, S., Rafiq, A., Al-Hussain, S. A., Zaki, M. E. A. 2024. *A Comprehensive Update of Anti-COVID-19 Activity of Heterocyclic Compounds.* Drug Des Devel Ther, 18(1547-1571.

[13] M.J. Frisch, G. W. T., H.B. Schlegel, G.E. Scuseria, M.A. Robb, J.R. Cheeseman, G. Scalmani, V. Barone, B. Mennucci, G.A. Petersson, H. Nakatsuji, M. Caricato, X. Li, H.P. Hratchian, A.F. Izmaylov, J. Bloino, G. Zheng, J.L. Sonnenberg, M. Hada, M. Ehara, K. Toyota, R. Fukuda, J. Hasegawa, M. Ishida, T. Nakajima, Y. Honda, O. Kitao, H. Nakai, T. Vreven, J.A. Montgomery Jr., J.E. Peralta, F. Ogliaro, M. Bearpark, J.J. Heyd, E. Brothers, K.N. Kudin, V.N. Staroverov, R. Kobayashi, J. Normand, K. Raghavachari, A. Rendell, J.C. Burant, S.S. Iyengar, J. Tomasi, M. Cossi, N. Rega, J.M. Millam, M. Klene, J.E. Knox, J.B. Cross, V. Bakken, C. Adamo, J. Jaramillo, R. Gomperts, R.E. Stratmann, O. Yazyev, A.J. Austin, R. Cammi, C. Pomelli, J.W. Ochterski, R.L. Martin, K. Morokuma, V.G. Zakrzewski, G.A. Voth, P. Salvador, J.J. Dannenberg, S. Dapprich, A.D. Daniels, Ö. Farkas, J.B. Foresman, J.V. Ortiz, J. Cioslowski, D.J. Fox, *Gaussian 09*. 2009.

[14] Burley, S. K., Berman, H. M., Bhikadiya, C., Bi, C., Chen, L., Di Costanzo, L., Christie, C., Dalenberg, K., Duarte, J. M., Dutta, S. 2019. *RCSB Protein Data Bank: biological macromolecular structures enabling research and education in fundamental biology, biomedicine, biotechnology and energy.* Nucleic acids research, 47(D1), D464-D474.

[15] Release, S., *1: Maestro, Schrodinger, LLC, New York*. 2019.

[16] ULC, C. C. G., *Molecular Operating Environment (MOE)*. 2019, Chemical Computing Group ULC: Montreal, QC, Canada.

[17] BIOVIA, D. S., *Discovery Studio Visualizer*, in *Dassault Systèmes*, C. San Diego, USA, Editor. 2016.

[18] Gören, K., Bağlan, M., Yıldıko, Ü. 2025. *Analysis By Dft, Adme And Docking Studies Of N'-(4-Hydroxy-3-Methoxybenzylidene)Naphtho[2,3-B]Furan-2-Carbohydrazide.* Eskişehir Teknik Üniversitesi Bilim ve Teknoloji Dergisi B - Teorik Bilimler, 13(1), 7-23.

[19] Tahiroğlu, V., Gören, K., Yıldıko, Ü., Bağlan, M. 2024. *IInvestigation, Structural Characterization and Evaluation of the Biological Potency by Molecular Docking of Amoxicillin Analogue of a Schiff Base Molecule.* International Journal of Chemistry and Technology, 8(2), 190-199.

[20] Gören, K., Bağlan, M., Tahiroğlu, V., Yıldıko, Ü. 2024. *Theoretical Calculations and Molecular Docking Analysis of 4-(2-(4-Bromophenyl)Hydrazineylidene)-3,5-Diphenyl-4H-Pyrazole Molecule.* Journal of Advanced Research in Natural and Applied Sciences, 10(4), 786-802.

[21] Gören, K., Bağlan, M., Yıldıko, Ü. 2024. *Antimicrobial, and Antitubercular Evaluation with*

ADME and Molecular Docking Studies and DFT Calculatıons of (Z)-3-((1-(5-amino-1,3,4-thiadiazol-2-yl)-2-Phenylethyl)imino)-5-nitroindolin-2-one Schiff Base. Karadeniz Fen Bilimleri Dergisi, 14(4), 1694-1708.

[22] Zreigh, M. M., Adams, H., Jackson, R. F. W., Robertson, C. C. 2019. *The first crystal structure of the pyrrolo-[1,2-c]oxazole ring system.* Acta Crystallogr E Crystallogr Commun, 75(Pt 9), 1336-1338.

[23] Bahjou, Y., Draoui, Y., Radi, S., Robeyns, K., Li, W., Miras, H. N., Ferbinteanu, M., Rotaru, A., Bittner, H., Jakupec, M. A. 2026. *Coordination Complexes and Polymers of Novel Hybrid Tetrazole-Triazole-Pyrazole Ligands: Synthesis, Structural Characterization, and Biological Evaluation.* Chemistry–A European Journal, e02238.

[24] Gören, K., Bağlan, M., Yıldıko, Ü. 2024. *Melanoma Cancer Evaluation with ADME and Molecular Docking Analysis, DFT Calculations of (E)-methyl 3-(1-(4-methoxybenzyl)-2,3-dioxoindolin-5-yl)-acrylate Molecule.* Journal of the Institute of Science and Technology, 14(3), 1186-1199.

[25] Tahiroğlu, V., Gören, K., Çimen, E., Yıldıko, Ü. 2024. *Moleculer Docking and Theoretical Analysis of the (E)-5-((Z)-4-methylbenzylidene)-2-(((E)-4-methylbenzylidene)hydrazineylidene)-3-phenylthiazolidin-4-one Molecule.* Bitlis Eren Üniversitesi Fen Bilimleri Dergisi, 13(3), 659-672.

[26] Hussein, H. A. 2023. *A DFT study of structural-stability, Mulliken charges, MEP, FMO, and NLO properties of trans alkenyl substituted chalcones conformers: theoretical study.* Structural Chemistry, 34(6), 2201-2223.

[27] Shalaby, M. A., BinSabt, M. H., Rizk, S. A., Fahim, A. M. 2024. *Novel pyrazole and imidazolone compounds: synthesis, X-ray crystal structure with theoretical investigation of new pyrazole and imidazolone compounds anticipated insecticide's activities against targeting Plodia interpunctella and nilaparvata lugens.* RSC advances, 14(15), 10464-10480.

[28] Hossan, A., Aljohani, M., Alrefaei, A. F., Althumayri, K., Bayazeed, A., Saad, F. A., Abumelha, H. M., El-Metwaly, N. M. 2023. *Synthesis of functionalized aminopyrazole and pyrazolopyrimidine derivatives: Molecular modeling and docking as anticancer agents.* Arabian Journal of Chemistry, 16(4), 104645.

[29] Gören, K., Yıldıko, Ü. 2024. *Aldose Reductase Evaluation against Diabetic Complications Using ADME and Molecular Docking Studies and DFT Calculations of Spiroindoline Derivative Molecule.* Süleyman Demirel Üniversitesi Fen Bilimleri Enstitüsü Dergisi, 28(2), 281-292.

[30] Tahiroğlu, V., Gören, K., Bağlan, M., Yıldıko, Ü. 2024. *Molecular Docking and DFT Analysis of Thiazolidinone-Bis Schiff Base for anti-Cancer and anti-Urease Activity.* Journal of the Institute of Science and Technology, 14(2), 822-834.

[31] Bağlan, M., Gören, K., Yıldıko, Ü. 2023. *HOMO–LUMO, NBO, NLO, MEP analysis and molecular docking using DFT calculations in DFPA molecule.* International Journal of Chemistry and Technology, 7(1), 38-47.

[32] Jayaprakash, A., Arjunan, V., Jose, S. P., Mohan, S. 2011. *Vibrational and electronic investigations, thermodynamic parameters, HOMO and LUMO analysis on crotonaldehyde by ab initio and DFT methods.* Spectrochimica Acta Part A: Molecular and Biomolecular Spectroscopy, 83(1), 411-419.

[33] Saracoglu, M., Kokbudak, Z., Cimen, Z., Kandemirli, F. 2019. *Synthesis and DFT Quantum Chemical Calculations of Novel Pyrazolo [1, 5-c] pyrimidin-7 (1H)-one Derivatives.* Journal of the Chemical Society of Pakistan, 41(3),

[34] Sivakumar, C., Revathi, B., Balachandran, V., Narayana, B., Salian, V. V., Shanmugapriya, N., Vanasundari, K. 2021. *Molecular structure, spectroscopic, quantum chemical, topological, molecular docking and antimicrobial activity of 3-(4-Chlorophenyl)-5-[4-propan-2-yl) phenyl-4, 5-dihydro-1H-pyrazol-1-yl] (pyridin-4-yl) methanone.* Journal of Molecular Structure, 1224(129286.

[35] Bhagwat, S. K., Pawar, T. J., Kulkarni, S. A., Patil, A. A., More, R. A., Jimenez-Halla, J. O. C., Alvarado-Salazar, J. A., Olivares-Romero, J. L., Muteeb, G., Delgado-Alvarado, E. 2024. *Synthesis, characterization, biological activities, and computational studies of pyrazolyl–thiazole derivatives of thiophene.* RSC advances, 14(52), 39004-39016.

[36] Bağlan, M., Gören, K., Yıldıko, Ü. 2023. *DFT Computations and Molecular Docking Studies of 3-(6-(3-aminophenyl)thiazolo[1,2,4]triazol-2-yl)-2H-chromen-2-one(ATTC) Molecule.* Hittite Journal of Science and Engineering, 10(1), 11-19.

[37] Bağlan, M., Gören, K., Çakmak, İ. 2022. *Theoretical Investigation of 1H and 13C NMR Spectra of Diethanol Amine Dithiocarbamate RAFT Agent.* Journal of the Institute of Science and Technology, 12(3), 1677-1689.

[38] Ramazani, A., Sheikhi, M., Hanifehpour, Y., Asiabi, P. A., Joo, S. W. 2018. *Molecular Structure, Electronic Properties, Homo–Lumo, MEP and NBO Analysis of (N-Isocyanimino) Triphenylphosphorane (Ph3PNNC): DFT*

Calculations. Journal of Structural Chemistry, 59(3), 529-540.

[39] Celik, S. 2023. *DFT investigations and molecular docking as potent inhibitors of SARS-CoV-2 main protease of 4-phenylpyrimidine.* Journal of Molecular Structure, 1277(134895.

[40] Khowdiary, M. M., Khan, S., Iqbal, T., Rehman, W., Hayat, A., Hussain, R., Shaaer, N. A. L., Kashtoh, H. 2025. *Anti-Leukemic Profiling of Oxazole-Linked Oxadiazole Derivatives: A Computational and Kinetic Approach.* Pharmaceuticals, 18(5), 625.

[41] Abdo, M. A., Badawy, S. A., Fadda, A. A., Elmorsy, M. R. 2025. *Design, synthesis, structural characterization, and antioxidant potential of novel triazole- and oxadiazole-based hydrazide-hydrazone derivatives: spectroscopic, DFT, and molecular docking studies.* BMC Chemistry, 20(1), 19.

[42] Bağlan, M., Yıldıko, Ü., Gören, K. 2022. *Computational Investigation of 5.5'',7''-trihydroxy-3,7-dimethoxy-4'-4'''-O-biflavone from Flavonoids Using DFT Calculations and Molecular Docking.* Adıyaman University Journal of Science, 12(2), 283-298.

[43] Bağlan, M., Yıldıko, Ü., Gören, K. 2023. *DFT Calculations And Molecular Docking Study In 6-(2"-Pyrrolidinone-5"-Yl)-(-) Epicatechin Molecule From Flavonoids.* Eskişehir Teknik Üniversitesi Bilim ve Teknoloji Dergisi B - Teorik Bilimler, 11(1), 43-55.

[44] Tang, G., Zhao, J., Jiang, Z., Kou, S., Ju, X., Wei, C. 2012. *DFT and ab initio study on non-linear optical (NLO) properties of some organic complexes with different conjugate linker and substituent groups.* Optics and Spectroscopy, 113(3), 240-258.

[45] Tedjeuguim, C. T., Tasheh, S. N., Alongamo, C. I. L., Ghogomu, J. N. 2022. *A DFT and TD-DFT study of charge transport and non-linear optical properties of N-(4-methoxybenzylidene)isonicotinohydrazone, 2,2'-bipyridine and their Fe2+, Ni2+, Cu2+, Pd2+ and Pt2+ complexes.* Journal of Chemical Sciences, 134(3), 70.

[46] Irfan, M., Khan, H. A., Bibi, S., Wu, G., Ali, A., Khan, S. G., Alhokbany, N., Rasool, F., Chen, K. 2024. *Exploration of nonlinear optical properties of 4-methyl-4H-1,2,4-triazol-3-yl)thio)-N-phenylpropanamide based derivatives: experimental and DFT approach.* Scientific Reports, 14(1), 2732.

[47] Waddar, B., Gandi, S., Parne, S. R., Chari, V. R., Prasanth, G. R. 2024. *Investigation of second-order NLO properties of novel 1,3,4-oxadiazole derivatives: a DFT study.* J Mol Model, 30(5), 118.

[48] Halim, S. A., El-Meligy, A. B., El-Nahas, A. M., El-Demerdash, S. H. 2024. *DFT study, and natural bond orbital (NBO) population analysis of 2-(2-Hydroxyphenyl)-1-azaazulene tautomers and their mercapto analouges.* Scientific Reports, 14(1), 219.

[49] Paul, B. K., Guchhait, N. 2011. *Density functional theory (DFT) and natural bond orbital (NBO) investigation of intramolecular hydrogen bond interaction and excited-state intramolecular proton transfer (ESIPT) reaction in a five-membered hydrogen-bonding system 2-(1H-pyrazol-5-yl)pyridine: On the possibility of solvent (water)-assisted ESPT.* Computational and Theoretical Chemistry, 972(1), 1-13.

[50] Awad, M. K., Halim, W. S. A., Atlam, F. M., Fawzy, M. M. 2025. *A multiscale computational investigation for protection of carbon steel surface by pyrazolo-pyrimidine derivatives.* Scientific Reports, 15(1), 32576.

[51] Demir, S., Tinmaz, F., Dege, N., Ilhan, I. O. 2016. *Vibrational spectroscopic studies, NMR, HOMO–LUMO, NLO and NBO analysis of 1-(2-nitrobenzoyl)-3, 5-diphenyl-4, 5-dihydro-1H-pyrazole with use X-ray diffractions and DFT calculations.* Journal of Molecular Structure, 1108(637-648.

[52] Halim, S. A., Khalil, A. K. 2017. *TD-DFT calculations, NBO analysis and electronic absorption spectra of some thiazolo[3,2-a]pyridine derivatives.* Journal of Molecular Structure, 1147(651-667.

[53] Arı, H., Büyükmumcu, Z., Özpozan, T., İlhan, İ. Ö., Bahadır, Ö. 2013. *Vibrational and theoretical analysis of pentyl-4-benzoyl-1-[2, 4-dinitrophenyl]-5-phenyl-1H-pyrazole-3-carboxylate.* Spectrochimica Acta Part A: Molecular and Biomolecular Spectroscopy, 110(193-204.

[54] Erkan, S., Karakaş, D. 2019. *DFT investigation and molecular docking studies on dinuclear metal carbonyls containing pyridyl ligands with alkyne unit.* Chemical Papers, 73(10), 2387-2398.

[55] Shah, A., Parmar, G., Shah, U., Perumal, S. 2023. *Virtual Screening, Molecular Docking Studies and DFT Calculations of Novel Anticancer Flavonoids as Potential VEGFR-2 Inhibitors.* Chemistry Africa, 6(4), 1847-1861.

[56] Karthick, R., Velraj, G., Pachamuthu, M. P., Karthikeyan, S. 2021. *Synthesis, spectroscopic, DFT, and molecular docking studies on 1,4-dihydropyridine derivative compounds: a combined experimental and theoretical study.* Journal of Molecular Modeling, 28(1), 5.

[57] Yele, V., Sigalapalli, D. K., Jupudi, S., Mohammed, A. A. 2021. *DFT calculation, molecular docking, and molecular dynamics simulation study on substituted phenylacetamide and benzohydrazide derivatives.* Journal of Molecular Modeling, 27(12), 359.

[58] Akhtar, M. N., AlDamen, M. A., Zierkiewicz, W., Michalczyk, M., Khalid, M., Idrisi, M., Shahid, M. 2020. *Synthesis, crystal structure, DFT calculations, molecular docking study and Hirshfeld surface analysis of alkoxido-bridged dinuclear iron(III) complex.* Research on Chemical Intermediates, 46(9), 4155-4171.

[59] Studio, B. D. 2016. *Dassault Systèmes Biovia Corporation.* San Diego, USA,

[60] Aycan, T., Öztürk, S., Demircioğlu, Z., Ersanlı, C. C. 2023. *Quantum Mechanical Calculations, Hirshfeld Surface Analysis, Molecular Docking, ADME and Toxicology Studies of the Ethyl 4-chloro-2-[(4-nitrophenyl)hydrazono]-3-oxobutrate Compound.* International Scientific and Vocational Studies Journal, 7(2), 109-121.

[61] Akocak, S. 2025. *Innovative Design, Synthesis, and In Silico Evaluation of Bis-Ureido Substituted Antipyrine Derivatives: Molecular Modeling and ADME Insights.* Journal of the Institute of Science and Technology, 15(1), 264-278.